

Measurement of the ratio of branching fractions

$$\mathcal{B}(B_c^+ \rightarrow J/\psi \tau^+ \nu_\tau) / \mathcal{B}(B_c^+ \rightarrow J/\psi \mu^+ \nu_\mu)$$

LHCb collaboration[†]

Abstract

A measurement is reported of the ratio of branching fractions $\mathcal{R}(J/\psi) = \mathcal{B}(B_c^+ \rightarrow J/\psi \tau^+ \nu_\tau) / \mathcal{B}(B_c^+ \rightarrow J/\psi \mu^+ \nu_\mu)$, where the τ^+ lepton is identified in the decay mode $\tau^+ \rightarrow \mu^+ \nu_\mu \bar{\nu}_\tau$. This analysis uses a sample of proton-proton collision data corresponding to 3.0 fb^{-1} of integrated luminosity recorded with the LHCb experiment at center-of-mass energies 7 TeV and 8 TeV. A signal is found for the decay $B_c^+ \rightarrow J/\psi \tau^+ \nu_\tau$ at a significance of 3 standard deviations, corrected for systematic uncertainty, and the ratio of the branching fractions is measured to be $\mathcal{R}(J/\psi) = 0.71 \pm 0.17 \text{ (stat)} \pm 0.18 \text{ (syst)}$. This result lies within 2 standard deviations above the range of existing predictions in the Standard Model.

Submitted to Phys. Rev. Lett.

© CERN on behalf of the LHCb collaboration, licence CC-BY-4.0.

[†]Authors are listed at the end of this letter.

18 Semileptonic b -hadron decays provide powerful probes for testing the Standard Model
 19 (SM) and for searching for the effects of physics beyond the SM. Due to their relatively
 20 simple theoretical description via tree-level processes in the SM, these decay modes serve as
 21 an ideal setting for examining the universality of the couplings of the three charged leptons
 22 in electroweak interactions. Recent measurements of the parameters $\mathcal{R}(D)$ and $\mathcal{R}(D^*)$,
 23 corresponding to the ratios of branching fractions $\mathcal{B}(B \rightarrow D^{(*)}\tau^-\bar{\nu}_\tau)/\mathcal{B}(B \rightarrow D^{(*)}\mu^-\bar{\nu}_\mu)$,
 24 by the BaBar [1, 2], Belle [3–6] and LHCb [7–9] collaborations indicate larger values than
 25 the SM predictions [10]. Proposed explanations for these discrepancies include extensions
 26 of the SM that involve enhanced weak couplings to third-generation leptons and quarks,
 27 such as interactions involving a charged Higgs boson [11, 12], leptoquarks [13], or new
 28 vector bosons [14]. Furthermore, other hints of the failure of lepton flavor universality
 29 have been seen in electroweak loop-induced B -meson decays [15, 16].

30 Measurements of semitauonic decays of other species of b hadrons can provide additional
 31 handles for investigating the sources of theoretical and experimental uncertainties, and
 32 potentially the origin of lepton nonuniversal couplings. This Letter presents the first study
 33 of the semitauonic decay $B_c^+ \rightarrow J/\psi \tau^+ \nu_\tau$ and a measurement of the ratio of branching
 34 fractions

$$\mathcal{R}(J/\psi) = \frac{\mathcal{B}(B_c^+ \rightarrow J/\psi \tau^+ \nu_\tau)}{\mathcal{B}(B_c^+ \rightarrow J/\psi \mu^+ \nu_\mu)}, \quad (1)$$

35 for which the current SM predictions are in the range of 0.25 to 0.28, where the spread
 36 arises from the choice of modeling approach for form factors [17–20]. Here and throughout
 37 the Letter charge-conjugate processes are implied.

38 The measurement is performed using data recorded with the LHCb detector at the
 39 Large Hadron Collider in 2011 and 2012, corresponding to integrated luminosities of 1 fb^{-1}
 40 and 2 fb^{-1} collected at proton-proton (pp) center-of-mass energies of 7 TeV and 8 TeV,
 41 respectively. The analysis procedure is designed to identify both the signal decay chain
 42 $B_c^+ \rightarrow J/\psi \tau^+ \nu_\tau$ and the normalization mode $B_c^+ \rightarrow J/\psi \mu^+ \nu_\mu$, with $J/\psi \rightarrow \mu^+ \mu^-$ and
 43 $\tau^+ \rightarrow \mu^+ \nu_\mu \bar{\nu}_\tau$, through their identical visible final states $(\mu^+ \mu^-) \mu^+$. The muon candidate
 44 not originating from the J/ψ is referred to as the *unpaired* muon. The two modes
 45 are distinguished using differences in their kinematic properties. The selected sample
 46 contains contributions from the signal and the normalization modes, as well as several
 47 background processes. The contributions of the various components are determined from
 48 a multidimensional fit to the data, where each component is represented by a template
 49 distribution derived from control data samples or from simulation validated against data.
 50 The selection and fit procedures are developed without knowledge of the signal yield.

51 The LHCb detector is a single-arm forward spectrometer covering the pseudorapidity
 52 range $2 < \eta < 5$, described in detail in Refs. [21, 22]. Notably for this analysis, muons are
 53 identified by a system composed of alternating layers of iron and multiwire proportional
 54 chambers [23]. The online event selection is performed by a trigger [24], which in this
 55 case consists of a hardware stage, based on information from the calorimeter and muon
 56 systems, followed by a software stage, which applies a full event reconstruction. Simulated
 57 data samples, which are used for producing fit templates and evaluating the signal to
 58 normalization efficiency ratio, are produced using the software described in Refs. [25–28].

59 Events containing a $J/\psi \mu^+$ candidate are required to have been selected by the LHCb
 60 hardware dimuon trigger, with both muon candidates at the trigger level matched to the
 61 decay products of the J/ψ candidate in the offline selection. In the software trigger, the
 62 events are required to meet criteria designed to select $J/\psi \rightarrow \mu^- \mu^+$ candidates constructed

63 from oppositely charged tracks whose particle identification information is consistent with
64 a muon. The J/ψ candidate must have $p_T > 2 \text{ GeV}/c$, where p_T is the component of the
65 momentum transverse to the beam, and have a reconstructed mass consistent with the
66 known J/ψ mass [29]. In addition, the momenta of the J/ψ decay products must each
67 exceed $5 \text{ GeV}/c$ and at least one muon candidate must have $p_T > 1.5 \text{ GeV}/c$.

68 Further requirements are imposed in the offline selection. The unpaired muon candidate
69 must have $p_T > 750 \text{ MeV}/c$ and be detached from any primary vertex (PV). The J/ψ
70 candidate is required to have well-identified muon decay products, to have a decay vertex
71 significantly separated from any PV in the event, and to have an invariant mass within
72 $55 \text{ MeV}/c^2$ of the known J/ψ mass. The unpaired muon candidate is required to satisfy
73 muon identification criteria, have a momentum in the range $3 < p < 100 \text{ GeV}/c$, be in the
74 pseudorapidity range 2 to 5, be significantly separated from any PV, and form a vertex
75 with the J/ψ candidate. A veto is applied to exclude candidates in which the invariant
76 mass of the opposite-sign muon pair formed by swapping the unpaired muon with a
77 muon from the J/ψ candidate is consistent with the J/ψ mass. To suppress combinatorial
78 background constructed from the decay products of other b hadrons in the event, the
79 J/ψ and the unpaired μ candidates must not have momenta pointing in nearly opposite
80 directions in the plane transverse to the beam axis. Additional requirements are imposed
81 to ensure good-quality tracks. In the rare ($< 2\%$) events where more than one candidate
82 is selected, a single candidate is retained randomly but reproducibly.

83 The $J/\psi \mu^+$ candidates from partially reconstructed b -hadron decays, including B_c^+
84 decays to a $J/\psi H_c$ pair, where H_c stands for a charmed hadron, and semileptonic $B_c^+ \rightarrow$
85 $J/\psi (n\pi)\mu^+\nu_\mu$ decays with $n \geq 2$, are typically accompanied by additional nearby charged
86 particles. In order to suppress these background contributions, candidates are required to
87 be isolated from additional tracks in the event based on a boosted decision tree (BDT)
88 described in Ref. [7]. The algorithm assigns a score based on whether a given track is
89 likely to have originated from the signal B_c^+ candidate or from the rest of the event.
90 The signal sample is constructed by requiring that no tracks in the event are consistent
91 with originating from the B_c^+ candidate, based on their BDT response value, and is thus
92 enriched in $B_c^+ \rightarrow J/\psi \tau^+ \nu_\tau$ and $B_c^+ \rightarrow J/\psi \mu^+ \nu_\mu$ decays.

93 The selection efficiencies for the signal and normalization modes are determined from
94 simulation. To account for the effect of differing detector occupancy and resolution
95 between simulation and data, the joint distributions of the track multiplicity and the
96 significances of the separation of the J/ψ and of the unpaired muon from the associated
97 PV (defined to be the PV with respect to which the particle has the smallest impact
98 parameter χ^2 , which is the difference in χ^2 of the PV fit with and without the particle
99 in question) in the simulated samples are weighted to match the observed distribution
100 in a subset of the data sample enriched in the normalization mode, without biasing the
101 simulated decay time distribution [30]. The ratio of the signal efficiency to that of the
102 normalization mode is found to be $(52.4 \pm 0.4)\%$, where the uncertainty reflects the limited
103 size of the simulation samples.

104 The differences in the kinematic distributions of the various processes are exploited to
105 disentangle their respective contributions to the selected $J/\psi \mu^+$ sample. The large μ - τ
106 mass difference and the presence of extra neutrinos from the decay $\tau^+ \rightarrow \mu^+ \nu_\mu \bar{\nu}_\tau$ result in
107 distinct distributions for the signal relative to the normalization mode. Three kinematic
108 quantities are used: the unpaired-muon energy in the B_c^+ rest frame, E_μ^* ; the missing mass
109 squared, defined as $m_{\text{miss}}^2 = (p_{B_c^+} - p_{J/\psi} - p_\mu)^2$; and the squared four-momentum transfer to

110 the lepton system, $q^2 = (p_{B_c^+} - p_{J/\psi})^2$, where $p_{B_c^+}$, $p_{J/\psi}$ and p_μ are the four-momenta of
 111 the B_c^+ meson, the J/ψ meson, and the unpaired muon, respectively. These quantities are
 112 approximated using a technique developed in Ref. [7] that estimates the B_c^+ momentum
 113 despite the presence of one or more missing neutrinos, using the flight direction of the
 114 candidate, determined from the vector joining the associated PV and the decay vertex, and
 115 the momenta of its decay products. The lifetime of the B_c^+ meson, which is nearly three
 116 times shorter than that of other b hadrons, provides an additional handle for discriminating
 117 against the large background that originates from lighter b hadrons. The decay time for
 118 each $J/\psi \mu^+$ candidate is computed using the decay distance of the candidate, determined
 119 from the approximated B_c^+ momentum vector and the displacement of its reconstructed
 120 vertex relative to its associated PV. Decay-time distributions derived from simulation are
 121 corrected for acceptance differences between data and simulation. This is achieved by
 122 applying weights to the simulated distribution from a study of a control sample of $J/\psi K^+$
 123 combinations from the decay $B^0 \rightarrow J/\psi K^*(892)^0$, with $K^*(892)^0 \rightarrow K^+ \pi^-$, in data and
 124 simulation.

125 The contributions of various components to the sample of $J/\psi \mu^+$ candidates are
 126 represented by three-dimensional histogram templates, binned in m_{miss}^2 , the decay time
 127 of the B_c^+ candidate, and a discrete quantity Z , representing eight bins in (E_μ^*, q^2) . The
 128 values 0–3 of Z correspond to bins where $q^2 < 7.15 \text{ GeV}^2/c^4$ and E_μ^* is divided with
 129 thresholds at $[0.68, 1.15, 1.64] \text{ GeV}$. The values 4–7 correspond to bins with the same E_μ^*
 130 ranges, but where $q^2 \geq 7.15 \text{ GeV}^2/c^4$.

131 The templates are derived from simulation for the signal and the normalization modes,
 132 which requires knowledge of the $B_c^+ \rightarrow J/\psi \ell^+ \nu_\ell$ form factors. These have not yet been
 133 precisely determined and the theoretical predictions, *e.g.* those from Refs. [18] and [31],
 134 are yet to be tested against data. Thus, for this measurement, the shared form factors for
 135 the signal and normalization modes are determined directly from the data by employing a
 136 z -expansion parametrization inspired by Ref. [32] to fit a subsample of the data that is
 137 enriched in the normalization mode. In this expansion, the form factors $V(q^2)$, $A_0(q^2)$,
 138 $A_1(q^2)$, and $A_2(q^2)$ (following the convention of Ref. [31]) are fit by functions of the form

$$f(q^2) = \frac{1}{1 - q^2/M_{\text{pole}}^2} \sum_{k=0}^K a_k z(q^2)^k, \quad (2)$$

139 where $z(q^2)$ is defined in Ref. [32]. The pole mass M_{pole} is the mass of the excited B_c^+
 140 state with quantum numbers corresponding to the form factor: the $J^P = 1^-$ state for
 141 $V(q^2)$, taken to be $6.33 \text{ GeV}/c^2$; the 0^- state for $A_0(q^2)$, which is the B_c^+ mass itself; and
 142 finally the 1^+ state for $A_1(q^2)$ and $A_2(q^2)$, taken to be $6.73 \text{ GeV}/c$ [18, 31]. The form
 143 factor $A_0(q^2)$ is fit to $K = 0$ order, while the others are fit to the linear $K = 1$ order.
 144 The parameters obtained from this procedure contain the effects of the reconstruction
 145 resolution of the kinematic parameters and cannot be directly compared with existing
 146 theoretical predictions.

147 Simulation is used to determine the templates for the feed-down processes $B_c^+ \rightarrow$
 148 $\psi(2S)\mu^+\nu_\mu$, $B_c^+ \rightarrow \psi(2S)\tau^+\nu_\tau$, $B_c^+ \rightarrow \chi_{c1}\mu^+\nu_\mu$, and $B_c^+ \rightarrow \chi_{c2}\mu^+\nu_\mu$, and backgrounds
 149 from $B_c^+ \rightarrow J/\psi H_c X$. The last is represented by a cocktail of decays that result from $b \rightarrow$
 150 $c\bar{c}s$ transitions. The branching fractions for the decays $J/\psi \rightarrow \mu^+\mu^-$, $\psi(2S) \rightarrow J/\psi X$,
 151 $\chi_{c(1,2)} \rightarrow J/\psi \gamma$, and $\tau^+ \rightarrow \mu^+\nu_\mu\bar{\nu}_\tau$ are fixed to the known values [29]. A possible feed-
 152 down contribution from $B_c^+ \rightarrow X(3872)\mu^+\nu_\mu$, where the $X(3872)$ state decay produces a

153 J/ψ , is considered in the determination of the systematic uncertainties. The semimuonic
 154 B_c^+ decays to χ_{c1} and χ_{c2} modes are constrained to have the same branching fractions
 155 relative to the normalization mode, differing only due to the respective branching fractions
 156 of $\chi_{c(1,2)}$ to $J/\psi\gamma$, consistent with theoretical expectations [33]. Form factors for these
 157 decays are taken from Ref. [33]. The rare semimuonic decay to χ_{c0} (suppressed by the
 158 low $\chi_{c0} \rightarrow J/\psi X$ branching fraction) and semitauonic decays involving χ_c states are
 159 neglected and are accounted for in the systematic uncertainties.

160 The background processes $B_c^+ \rightarrow J/\psi H_c X$ are modeled using a cocktail of two-body
 161 decays and quasi-two-body decays that proceed through excited D_s^+ resonances. Several
 162 decay modes in the cocktail have recently been measured at LHCb [34], and for others the
 163 branching fractions are fixed by analogy to the well measured $B \rightarrow D^* H_c X$ decays [29].
 164 The cocktail consists of the two-body and quasi-two-body decays in equal proportion.

165 The combinatorial background in the selected $J/\psi\mu^+$ sample is predominantly due to
 166 J/ψ mesons from $B_{u,d,s} \rightarrow J/\psi X$ decays paired with muon candidates from the rest of the
 167 event. This background source is modeled using a set of three template histograms taken
 168 from simulation for the three B -meson species, with their relative fractions constrained in
 169 accordance with the production cross-sections and their respective branching fractions.
 170 A fit is performed to the $J/\psi\mu^+$ mass distribution above $6.4 \text{ GeV}/c^2$, higher than the
 171 B_c^+ mass, to validate the modeling of this background and correct for possible sources
 172 of combinatorial background in data unaccounted for by the model, including decays
 173 of b baryons and the effect of unknown branching fractions. A linear correction to
 174 the $J/\psi\mu^+$ mass distribution in the simulation is determined by this fit and applied to
 175 the combinatorial background templates, and is varied within bounds to determine a
 176 systematic uncertainty.

177 The template for the background from combinatorial J/ψ candidates is determined
 178 using events where the J/ψ invariant mass lies above the nominal selection threshold,
 179 with its normalization fixed using a fit to the $\mu^+\mu^-$ invariant mass distribution. Two
 180 models for the shape of the combinatorial background in the J/ψ mass distribution are
 181 considered. The nominal fit uses a mixture of distributions with Gaussian cores and power
 182 law tails [35] for the true $J/\psi \rightarrow \mu^+\mu^-$ component and an exponential function for the
 183 combinatorial background. An alternative fit is performed to evaluate a corresponding
 184 systematic uncertainty.

185 The largest background component is due to the inclusive decays of light b hadrons to
 186 J/ψ mesons, in which an accompanying pion or kaon (or, less frequently, proton or electron)
 187 is misidentified as a muon, hereafter referred to as the mis-ID background. A data-driven
 188 approach is used to construct templates for this background component. A sample of $J/\psi h^+$
 189 candidates, where h^+ stands for a charged hadron, is selected following similar criteria to
 190 those of the signal sample, but with the h^+ failing the muon identification criteria. This
 191 control sample is enriched in various hadron and lepton species (primarily pions, kaons,
 192 and protons). Using several high-purity control samples of identified hadrons, weights
 193 are computed that represent the probability that a hadron with particular kinematic
 194 properties would pass the muon criteria. These weights are applied to the $J/\psi h^+$ sample to
 195 generate binned templates representing these background components. The normalization
 196 of each of these components is allowed to vary in the fit to the data.

197 A binned maximum likelihood (ML) fit is performed using the templates representing
 198 the various components, with their respective contributions and shape parameters corre-
 199 sponding to the B_c^+ lifetime and form factors allowed to vary. The contributions of the feed-

200 down processes involving the decays of higher-mass charmonium states, $B_c^+ \rightarrow \psi(2S)\mu^+\nu_\mu$,
 201 $B_c^+ \rightarrow \chi_{c(0,1,2)}(1P)\mu^+\nu_\mu$ are allowed to vary in the fit, whereas the ratio of the branch-
 202 ing fractions $\mathcal{R}(\psi(2S)) = \mathcal{B}(B_c^+ \rightarrow \psi(2S)\tau^+\nu_\tau)/\mathcal{B}(B_c^+ \rightarrow \psi(2S)\mu^+\nu_\mu)$ is fixed to the
 203 predicted SM value of 8.5% [18]. This is later varied for the evaluation of a systematic
 204 uncertainty.

205 Extensive studies of the fit procedure are carried out to identify potential sources of
 206 bias in the fit. Simulated signal is added to the data histograms, and the resulting changes
 207 in the value of $\mathcal{R}(J/\psi)$ from the fit are found to be consistent with the injected signal
 208 increments. The procedure is also applied to the mis-ID background, which shows no
 209 bias in the fitted number of events as a function of injected events. Another important
 210 consideration for this measurement is the disparate properties of the various templates.
 211 Some templates are populated in all kinematically allowed bins, such as the mis-ID
 212 background that is derived from large data samples. Others are sparsely populated and
 213 contain empty bins, *e.g.* for modes with low efficiency and yields that are obtained from
 214 simulated events. Pseudoexperiments with template compositions similar to those in this
 215 analysis reveal a possible bias of the fit results. Hence, the binning scheme for this analysis
 216 is chosen to minimize the number of empty bins in the sparsely populated templates,
 217 while retaining the discriminating power of the distributions. Kernel density estimation
 218 (KDE) [36] is used to derive continuous distributions representative of the nominal fit
 219 templates. Simulated pseudoexperiments using histogram templates sampled from these
 220 continuous distributions are then used to evaluate any remaining bias that results. Based
 221 on these studies a Bayesian procedure is implemented for correcting the raw $\mathcal{R}(J/\psi)$ value
 222 after unblinding.

223 The results of the fit are presented in Fig. 1, showing the projections of the nominal
 224 fit result onto the quantities m_{miss}^2 , decay time, and Z . The fit yields 1400 ± 300 signal
 225 and 19140 ± 340 normalization decays, where the errors are statistical and correlated.
 226 Accounting for the $\tau^+ \rightarrow \mu^+\nu_\mu\bar{\nu}_\tau$ branching fraction and the ratio of efficiencies gives an
 227 uncorrected value of 0.79 for $\mathcal{R}(J/\psi)$. Correcting for the mean expected bias at this value,
 228 we obtain $\mathcal{R}(J/\psi) = 0.71 \pm 0.17$ (stat). The significance of the signal, determined from a
 229 likelihood scan procedure and corrected for the systematic uncertainty, is found to be 3
 230 standard deviations.

231 Systematic uncertainties on $\mathcal{R}(J/\psi)$ are listed in Table 1. The effect of the limited
 232 size of the simulated samples on the template shapes is determined using the procedure
 233 of Refs. [37, 38]. In the nominal fit, the $B_c^+ \rightarrow J/\psi$ form factor parameters, except for
 234 the scalar form factor that primarily affects the semitaauonic mode, are fixed to the values
 235 obtained from a fit to a subset of the data enriched in the normalization mode. To assess
 236 the effect on $\mathcal{R}(J/\psi)$ due to this procedure, an alternative fit is performed with the form
 237 factor parameters allowed to vary, and the difference in quadrature of the uncertainties is
 238 assigned as a systematic uncertainty. The effect due to the $B_c^+ \rightarrow \psi(2S)$ form factors is
 239 evaluated by comparing fits using two different theoretical models for this template [18, 31].

240 The systematic uncertainty of the bias correction is calculated from the difference in
 241 bias between fits to simulated data based on a set of realistic parametrized distributions
 242 and corresponding fits based on KDE versions of these distributions. The effect of the
 243 binning of the quantity Z is determined by varying the boundaries of the thresholds in E_μ^*
 244 and q^2 , and by reducing the number of bins in the fit. A data-driven method is employed
 245 to determine the mis-ID background. In addition, an alternate approach is considered
 246 for modeling the effect of misreconstructed tracks. The fit procedure is performed with

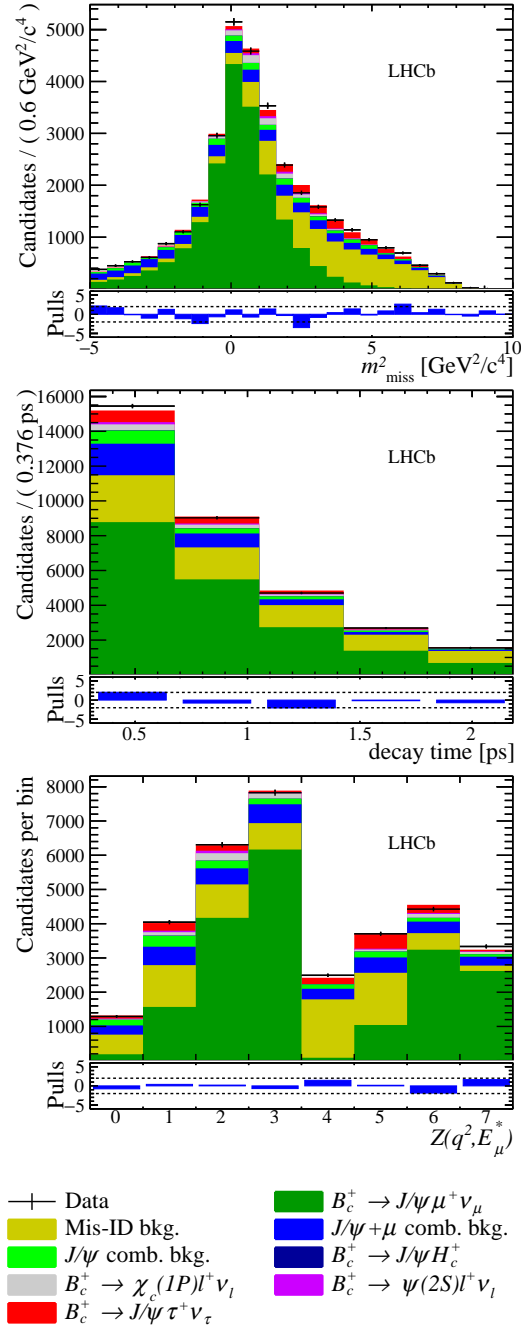


Figure 1: Distributions of (top) m_{miss}^2 , (middle) decay time, and (bottom) Z of the signal data, overlaid with projections of the fit model with all normalization and shape parameters at their best-fit values. Below each panel differences between the data and fit are shown, normalized by the Poisson uncertainty in the data; the dashed lines are at the values ± 2 .

247 templates derived from each of these methods, and an uncertainty is assigned using
 248 half the difference between the two minima. The systematic uncertainty due to the
 249 combinatorial background cocktail is determined by varying the linear correction made to
 250 its $J/\psi \mu^+$ mass distribution, described above, within its bounds. The contribution due
 251 to the combinatorial background in the J/ψ peak region is determined by varying the

Table 1: Systematic uncertainties in the determination of $\mathcal{R}(J/\psi)$.

Source of uncertainty	Size ($\times 10^{-2}$)
Limited size of simulation samples	8.0
$B_c^+ \rightarrow J/\psi$ form factors	12.1
$B_c^+ \rightarrow \psi(2S)$ form factors	3.2
Fit bias correction	5.4
Z binning strategy	5.6
Misidentification background strategy	5.6
Combinatorial background cocktail	4.5
Combinatorial J/ψ sideband scaling	0.9
$B_c^+ \rightarrow J/\psi H_c X$ contribution	3.6
Semitaonic $\psi(2S)$ and χ_c feed-down	0.9
Weighting of simulation samples	1.6
Efficiency ratio	0.6
$\mathcal{B}(\tau^+ \rightarrow \mu^+ \nu_\mu \bar{\nu}_\tau)$	0.2
B_c^+ lifetime	included in statistical uncertainty
Total systematic uncertainty	17.7
Statistical uncertainty	17.3

252 normalization of this component within the range determined from the alternative fits to
 253 the invariant-mass distribution of J/ψ candidates.

254 The systematic uncertainty due to the loosely constrained contribution of the process
 255 $B_c^+ \rightarrow J/\psi H_c X$ is determined by constraining the yield to that expected from the
 256 estimated branching fraction for these decays [29, 34]. The effect of the fixed contribution
 257 of the semitaonic decay $B_c^+ \rightarrow \psi(2S)\tau^+\nu_\mu$ is determined by varying $\mathcal{R}(\psi(2S))$ by $\pm 50\%$
 258 of the predicted value. Background from the feed-down decays $B_c^+ \rightarrow X(3872)\mu^+\nu_\mu$, with
 259 the principal decay chains $X(3872) \rightarrow J/\psi\pi^+\pi^-$ and $X(3872) \rightarrow J/\psi\gamma$, is kinematically
 260 similar to the background from $B_c^+ \rightarrow \psi(2S)\tau^+\nu_\mu$. An approximate bound on the number
 261 of $X(3872)$ candidates in the sample is obtained from the invariant mass distribution of
 262 $J/\psi\pi^+\pi^-$ combinations in the sample. This bound is found to be less than the uncertainty
 263 in the $\psi(2S)$ yield, and thus no additional uncertainty is assigned. The effect of the small
 264 contribution of semitaonic decays involving χ_c states is assessed by assuming that the
 265 entire yield for this mode is absorbed in the signal mode, and is summed in quadrature
 266 with that from the $\psi(2S)$ feed-down mode.

267 The systematic uncertainty due to the weighting of the simulation distributions of
 268 event parameters (the track multiplicity and the separation significances of the J/ψ and of
 269 the unpaired muon) is determined by varying the criteria for the definition of the subset of
 270 the data sample enriched in the normalization mode used in the weighting procedure, and
 271 employing alternative methods to account for the misidentified muon candidates in the
 272 sample. The uncertainty in the efficiency ratio measured in simulation is propagated to
 273 $\mathcal{R}(J/\psi)$. The B_c^+ lifetime is allowed to vary in the fit, constrained to its measured value
 274 and precision, and this effect is included in the statistical uncertainty of the measurement.

275 In summary, the decay $B_c^+ \rightarrow J/\psi\tau^+\nu_\tau$ is studied using data corresponding to 3 fb^{-1}
 276 recorded with the LHCb detector during 2011 and 2012, leading to the first measurement

277 of the ratio of branching fractions

$$\mathcal{R}(J/\psi) = \frac{\mathcal{B}(B_c^+ \rightarrow J/\psi \tau^+ \nu_\tau)}{\mathcal{B}(B_c^+ \rightarrow J/\psi \mu^+ \nu_\mu)} = 0.71 \pm 0.17 (\text{stat}) \pm 0.18 (\text{syst}). \quad (3)$$

278 This result lies within 2 standard deviations of the range of existing predictions in the
279 Standard Model, 0.25 to 0.28, assuming lepton universality.

280 Acknowledgements

281 We express our gratitude to our colleagues in the CERN accelerator departments for the
282 excellent performance of the LHC. We thank the technical and administrative staff at the
283 LHCb institutes. We acknowledge support from CERN and from the national agencies:
284 CAPES, CNPq, FAPERJ and FINEP (Brazil); MOST and NSFC (China); CNRS/IN2P3
285 (France); BMBF, DFG and MPG (Germany); INFN (Italy); NWO (The Netherlands);
286 MNiSW and NCN (Poland); MEN/IFA (Romania); MinES and FASO (Russia); MinECo
287 (Spain); SNSF and SER (Switzerland); NASU (Ukraine); STFC (United Kingdom); NSF
288 (USA). We acknowledge the computing resources that are provided by CERN, IN2P3
289 (France), KIT and DESY (Germany), INFN (Italy), SURF (The Netherlands), PIC (Spain),
290 GridPP (United Kingdom), RRCKI and Yandex LLC (Russia), CSCS (Switzerland), IFIN-
291 HH (Romania), CBPF (Brazil), PL-GRID (Poland) and OSC (USA). We are indebted to
292 the communities behind the multiple open-source software packages on which we depend.
293 Individual groups or members have received support from AvH Foundation (Germany),
294 EPLANET, Marie Skłodowska-Curie Actions and ERC (European Union), ANR, Labex
295 P2IO, ENIGMASS and OCEVU, and Région Auvergne-Rhône-Alpes (France), RFBR and
296 Yandex LLC (Russia), GVA, XuntaGal and GENCAT (Spain), Herchel Smith Fund, the
297 Royal Society, the English-Speaking Union and the Leverhulme Trust (United Kingdom).

298 References

- 299 [1] BaBar collaboration, J. P. Lees *et al.*, *Evidence for an excess of $\bar{B} \rightarrow D^{(*)} \tau^- \bar{\nu}_\tau$*
300 *decays*, Phys. Rev. Lett. **109** (2012) 101802, [arXiv:1205.5442](#).
- 301 [2] BaBar collaboration, J. P. Lees *et al.*, *Measurement of an excess of $\bar{B} \rightarrow D^{(*)} \tau^- \bar{\nu}_\tau$*
302 *decays and implications for charged Higgs bosons*, Phys. Rev. **D88** (2013) 072012,
303 [arXiv:1303.0571](#).
- 304 [3] Belle collaboration, M. Huschle *et al.*, *Measurement of the branching ratio of $\bar{B} \rightarrow$*
305 *$D^{(*)} \tau^- \bar{\nu}_\tau$ relative to $\bar{B} \rightarrow D^{(*)} \ell^- \bar{\nu}_\ell$ decays with hadronic tagging at Belle*, Phys. Rev.
306 **D92** (2015) 072014, [arXiv:1507.03233](#).
- 307 [4] Belle collaboration, Y. Sato *et al.*, *Measurement of the branching ratio of $\bar{B}^0 \rightarrow$*
308 *$D^{*+} \tau^- \bar{\nu}_\tau$ relative to $\bar{B}^0 \rightarrow D^{*+} \ell^- \bar{\nu}_\ell$ decays with a semileptonic tagging method*, Phys.
309 Rev. **D94** (2016) 072007, [arXiv:1607.07923](#).
- 310 [5] Belle collaboration, S. Hirose *et al.*, *Measurement of the τ lepton polarization*
311 *and $R(D^*)$ in the decay $\bar{B} \rightarrow D^* \tau^- \bar{\nu}_\tau$* , Phys. Rev. Lett. **118** (2017) 211801,
312 [arXiv:1612.00529](#).

- 313 [6] Belle collaboration, S. Hirose *et al.*, *Measurement of the τ lepton polarization*
314 *and $R(D^*)$ in the decay $\bar{B} \rightarrow D^* \tau^- \bar{\nu}_\tau$ with one-prong hadronic τ decays at Belle,*
315 *arXiv:1709.00129.*
- 316 [7] LHCb collaboration, R. Aaij *et al.*, *Measurement of the ratio of branching frac-*
317 *tions $\mathcal{B}(\bar{B}^0 \rightarrow D^{*+} \tau^- \bar{\nu}_\tau) / \mathcal{B}(\bar{B}^0 \rightarrow D^{*+} \mu^- \bar{\nu}_\mu)$,* Phys. Rev. Lett. **115** (2015) 111803,
318 *arXiv:1506.08614.*
- 319 [8] LHCb collaboration, R. Aaij *et al.*, *Measurement of the ratio of the $\mathcal{B}(B^0 \rightarrow$*
320 *$D^{*-} \tau^+ \nu_\tau)$ and $\mathcal{B}(B^0 \rightarrow D^{*-} \mu^+ \nu_\mu)$ branching fractions using three-prong τ -lepton*
321 *decays,* arXiv:1708.08856, submitted to Phys. Rev. Lett.
- 322 [9] LHCb collaboration, R. Aaij *et al.*, *Measurement of the $\mathcal{B}(B^0 \rightarrow D^{*-} \tau^+ \nu_\tau)$ branching*
323 *fraction using three-prong τ decays,* arXiv:1711.02505, submitted to Phys. Rev. D.
- 324 [10] Heavy Flavor Averaging Group, Y. Amhis *et al.*, *Averages of b -hadron, c -hadron,*
325 *and τ -lepton properties as of summer 2016,* arXiv:1612.07233, updated results and
326 plots available at <http://www.slac.stanford.edu/xorg/hflav/>.
- 327 [11] M. Tanaka, *Charged Higgs effects on exclusive semitauonic B decays,* Z. Phys. C **67**
328 (1995) 321, arXiv:hep-ph/9411405.
- 329 [12] A. Crivellin, C. Greub, and A. Kokulu, *Explaining $B \rightarrow D \tau \nu$, $B \rightarrow D^* \tau \nu$ and*
330 *$B \rightarrow \tau \nu$ in a two Higgs doublet model of type III,* Phys. Rev. **D86** (2012) 054014,
331 arXiv:1206.2634.
- 332 [13] M. Freytsis, Z. Ligeti, and J. T. Ruderman, *Flavor models for $\bar{B} \rightarrow D^{(*)} \tau \bar{\nu}$,* Phys.
333 Rev. **D92** (2015) 054018, arXiv:1506.08896.
- 334 [14] A. Crivellin, G. D'Ambrosio, and J. Heeck, *Addressing the LHC flavor anomalies with*
335 *horizontal gauge symmetries,* Phys. Rev. **D91** (2015) 075006, arXiv:1503.03477.
- 336 [15] LHCb collaboration, R. Aaij *et al.*, *Test of lepton universality using $B^+ \rightarrow K^+ \ell^+ \ell^-$*
337 *decays,* Phys. Rev. Lett. **113** (2014) 151601, arXiv:1406.6482.
- 338 [16] LHCb collaboration, R. Aaij *et al.*, *Test of lepton universality with $B^0 \rightarrow K^{*0} \ell^+ \ell^-$*
339 *decays,* JHEP **08** (2017) 055, arXiv:1705.05802.
- 340 [17] A. Yu. Anisimov, I. M. Narodetskii, C. Semay, and B. Silvestre-Brac, *The B_c meson*
341 *lifetime in the light-front constituent quark model,* Phys. Lett. **B452** (1999) 129,
342 arXiv:hep-ph/9812514.
- 343 [18] V. V. Kiselev, *Exclusive decays and lifetime of B_c^+ meson in QCD sum rules,*
344 arXiv:hep-ph/0211021.
- 345 [19] M. A. Ivanov, J. G. Korner, and P. Santorelli, *Exclusive semileptonic and nonleptonic*
346 *decays of the B_c meson,* Phys. Rev. **D73** (2006) 054024, arXiv:hep-ph/0602050.
- 347 [20] E. Hernández, J. Nieves, and J. M. Verde-Velasco, *Study of exclusive semileptonic*
348 *and non-leptonic decays of B_c^- in a nonrelativistic quark model,* Phys. Rev. **D74**
349 (2006) 074008, arXiv:hep-ph/0607150.

- 350 [21] LHCb collaboration, A. A. Alves Jr. *et al.*, *The LHCb detector at the LHC*, JINST **3**
351 (2008) S08005.
- 352 [22] LHCb collaboration, R. Aaij *et al.*, *LHCb detector performance*, Int. J. Mod. Phys.
353 **A30** (2015) 1530022, arXiv:1412.6352.
- 354 [23] A. A. Alves Jr. *et al.*, *Performance of the LHCb muon system*, JINST **8** (2013)
355 P02022, arXiv:1211.1346.
- 356 [24] R. Aaij *et al.*, *The LHCb trigger and its performance in 2011*, JINST **8** (2013) P04022,
357 arXiv:1211.3055.
- 358 [25] T. Sjöstrand, S. Mrenna, and P. Skands, *PYTHIA 6.4 physics and manual*, JHEP
359 **05** (2006) 026, arXiv:hep-ph/0603175; T. Sjöstrand, S. Mrenna, and P. Skands,
360 *A brief introduction to PYTHIA 8.1*, Comput. Phys. Commun. **178** (2008) 852,
361 arXiv:0710.3820.
- 362 [26] I. Belyaev *et al.*, *Handling of the generation of primary events in Gauss, the LHCb*
363 *simulation framework*, J. Phys. Conf. Ser. **331** (2011) 032047.
- 364 [27] C.-H. Chang, J.-X. Wang, and X.-G. Wu, *BCVEGPY2.0: A Upgrade version of the*
365 *generator BCVEGPY with an addendum about hadroproduction of the P-wave B(c)*
366 *states*, Comput. Phys. Commun. **174** (2006) 241, arXiv:hep-ph/0504017.
- 367 [28] Geant4 collaboration, J. Allison *et al.*, *Geant4 developments and applications*, IEEE
368 Trans. Nucl. Sci. **53** (2006) 270; Geant4 collaboration, S. Agostinelli *et al.*, *Geant4:*
369 *A simulation toolkit*, Nucl. Instrum. Meth. **A506** (2003) 250.
- 370 [29] Particle Data Group, C. Patrignani *et al.*, *Review of particle physics*, Chin. Phys.
371 **C40** (2016) 100001, and 2017 update.
- 372 [30] A. Rogozhnikov, *Reweighting with Boosted Decision Trees*, J. Phys. Conf. Ser. **762**
373 (2016), no. 1 012036, arXiv:1608.05806.
- 374 [31] D. Ebert, R. N. Faustov, and V. O. Galkin, *Weak decays of the B_c meson to*
375 *charmonium and D mesons in the relativistic quark model*, Phys. Rev. **D68** (2003)
376 094020, arXiv:hep-ph/0306306.
- 377 [32] C. Bourrely, I. Caprini, and L. Lellouch, *Model-independent description of $B \rightarrow \pi \ell \nu$*
378 *decays and a determination of $|V_{ub}|$* , Phys. Rev. **D79** (2009) 013008, Erratum *ibid.*
379 **D82** (2010) 099902, arXiv:0807.2722.
- 380 [33] X. X. Wang, W. Wang, and C. D. Lü, *B_c to p-wave charmonia transitions in covariant*
381 *light-front approach*, Phys. Rev. **D79** (2009) 114018, arXiv:0901.1934.
- 382 [34] LHCb collaboration, R. Aaij *et al.*, *Observation of $B_c^+ \rightarrow J/\psi D_s^+$ and $B_c^+ \rightarrow J/\psi D_s^{*+}$*
383 *decays*, Phys. Rev. **D87** (2013) 112012, arXiv:1304.4530.
- 384 [35] T. Skwarnicki, *A study of the radiative cascade transitions between the Upsilon-prime*
385 *and Upsilon resonances*, PhD thesis, Institute of Nuclear Physics, Krakow, 1986,
386 DESY-F31-86-02.

- 387 [36] K. S. Cranmer, *Kernel estimation in high-energy physics*, Comput. Phys. Commun.
388 **136** (2001) 198, [arXiv:hep-ex/0011057](#).
- 389 [37] R. J. Barlow and C. Beeston, *Fitting using finite Monte Carlo samples*, Comput.
390 Phys. Commun. **77** (1993) 219.
- 391 [38] ROOT collaboration, K. Cranmer *et al.*, *HistFactory: A tool for creating statistical*
392 *models for use with RooFit and RooStats*, Tech. Rep. CERN-OPEN-2012-016, Jan,
393 2012.

LHCb collaboration

394 R. Aaij⁴⁰, B. Adeva³⁹, M. Adinolfi⁴⁸, Z. Ajaltouni⁵, S. Akar⁵⁹, J. Albrecht¹⁰, F. Alessio⁴⁰,
 395 M. Alexander⁵³, A. Alfonso Alberio³⁸, S. Ali⁴³, G. Alkhazov³¹, P. Alvarez Cartelle⁵⁵,
 396 A.A. Alves Jr⁵⁹, S. Amato², S. Amerio²³, Y. Amhis⁷, L. An³, L. Anderlini¹⁸, G. Andreassi⁴¹,
 397 M. Andreotti^{17,g}, J.E. Andrews⁶⁰, R.B. Appleby⁵⁶, F. Archilli⁴³, P. d'Argent¹²,
 398 J. Arnau Romeu⁶, A. Artamonov³⁷, M. Artuso⁶¹, E. Aslanides⁶, M. Atzeni⁴², G. Auremma²⁶,
 399 M. Baalouch⁵, I. Babuschkin⁵⁶, S. Bachmann¹², J.J. Back⁵⁰, A. Badalov^{38,m}, C. Baesso⁶²,
 400 S. Baker⁵⁵, V. Balagura^{7,b}, W. Baldini¹⁷, A. Baranov³⁵, R.J. Barlow⁵⁶, C. Barschel⁴⁰,
 401 S. Barsuk⁷, W. Barter⁵⁶, F. Baryshnikov³², V. Batozskaya²⁹, V. Battista⁴¹, A. Bay⁴¹,
 402 L. Beaucourt⁴, J. Beddow⁵³, F. Bedeschi²⁴, I. Bediaga¹, A. Beiter⁶¹, L.J. Bel⁴³, N. Belyi⁶³,
 403 V. Bellee⁴¹, N. Belloli^{21,i}, K. Belous³⁷, I. Belyaev^{32,40}, E. Ben-Haim⁸, G. Bencivenni¹⁹,
 404 S. Benson⁴³, S. Beranek⁹, A. Berezhnoy³³, R. Bernet⁴², D. Berninghoff¹², E. Bertholet⁸,
 405 A. Bertolin²³, C. Betancourt⁴², F. Betti¹⁵, M.-O. Bettler⁴⁰, M. van Beuzekom⁴³,
 406 Ia. Bezshyiko⁴², S. Bifani⁴⁷, P. Billoir⁸, A. Birnkraut¹⁰, A. Bizzeti^{18,u}, M. Bjørn⁵⁷, T. Blake⁵⁰,
 407 F. Blanc⁴¹, S. Blusk⁶¹, V. Bocci²⁶, T. Boettcher⁵⁸, A. Bondar^{36,w}, N. Bondar³¹,
 408 I. Bordyuzhin³², S. Borghi⁵⁶, M. Borisyak³⁵, M. Borsato³⁹, F. Bossu⁷, M. Boubdir⁹,
 409 T.J.V. Bowcock⁵⁴, E. Bowen⁴², C. Bozzi^{17,40}, S. Braun¹², T. Britton⁶¹, J. Brodzicka²⁷,
 410 D. Brundu¹⁶, E. Buchanan⁴⁸, C. Buri⁵⁶, A. Bursche^{16,f}, J. Buytaert⁴⁰, W. Byczynski⁴⁰,
 411 S. Cadeddu¹⁶, H. Cai⁶⁴, R. Calabrese^{17,g}, R. Calladine⁴⁷, M. Calvi^{21,i}, M. Calvo Gomez^{38,m},
 412 A. Camboni^{38,m}, P. Campana¹⁹, D.H. Campora Perez⁴⁰, L. Capriotti⁵⁶, A. Carbone^{15,e},
 413 G. Carboni^{25,j}, R. Cardinale^{20,h}, A. Cardini¹⁶, P. Carniti^{21,i}, L. Carson⁵², K. Carvalho Akiba²,
 414 G. Casse⁵⁴, L. Cassina²¹, M. Cattaneo⁴⁰, G. Cavallero^{20,40,h}, R. Cenci^{24,t}, D. Chamont⁷,
 415 M.G. Chapman⁴⁸, M. Charles⁸, Ph. Charpentier⁴⁰, G. Chatzikonstantinidis⁴⁷, M. Chefdeville⁴,
 416 S. Chen¹⁶, S.F. Cheung⁵⁷, S.-G. Chitic⁴⁰, V. Chobanova^{39,40}, M. Chrzaszcz^{42,27}, A. Chubykin³¹,
 417 P. Ciambrone¹⁹, X. Cid Vidal³⁹, G. Ciezarek⁴³, P.E.L. Clarke⁵², M. Clemencic⁴⁰, H.V. Cliff⁴⁹,
 418 J. Closier⁴⁰, J. Cogan⁶, E. Cogneras⁵, V. Cogoni^{16,f}, L. Cojocariu³⁰, P. Collins⁴⁰, T. Colombo⁴⁰,
 419 A. Comerma-Montells¹², A. Contu⁴⁰, A. Cook⁴⁸, G. Coombs⁴⁰, S. Coquereau³⁸, G. Corti⁴⁰,
 420 M. Corvo^{17,g}, C.M. Costa Sobral⁵⁰, B. Couturier⁴⁰, G.A. Cowan⁵², D.C. Craik⁵⁸,
 421 A. Crocombe⁵⁰, M. Cruz Torres¹, R. Currie⁵², C. D'Ambrosio⁴⁰, F. Da Cunha Marinho²,
 422 E. Dall'Occo⁴³, J. Dalseno⁴⁸, A. Davis³, O. De Aguiar Francisco⁴⁰, K. De Bruyn⁴⁰,
 423 S. De Capua⁵⁶, M. De Cian¹², J.M. De Miranda¹, L. De Paula², M. De Serio^{14,d},
 424 P. De Simone¹⁹, C.T. Dean⁵³, D. Decamp⁴, L. Del Buono⁸, H.-P. Dembinski¹¹, M. Demmer¹⁰,
 425 A. Dendek²⁸, D. Derkach³⁵, O. Deschamps⁵, F. Dettori⁵⁴, B. Dey⁶⁵, A. Di Canto⁴⁰,
 426 P. Di Nezza¹⁹, H. Dijkstra⁴⁰, F. Dordei⁴⁰, M. Dorigo⁴⁰, A. Dosil Suárez³⁹, L. Douglas⁵³,
 427 A. Dovbnya⁴⁵, K. Dreimanis⁵⁴, L. Dufour⁴³, G. Dujany⁸, P. Durante⁴⁰, R. Dzhelezhyan³⁷,
 428 M. Dziewiecki¹², A. Dziurda⁴⁰, A. Dzyuba³¹, S. Easo⁵¹, M. Ebert⁵², U. Egede⁵⁵,
 429 V. Egorychev³², S. Eidelman^{36,w}, S. Eisenhardt⁵², U. Eitschberger¹⁰, R. Ekelhof¹⁰, L. Eklund⁵³,
 430 S. Ely⁶¹, S. Esen¹², H.M. Evans⁴⁹, T. Evans⁵⁷, A. Falabella¹⁵, N. Farley⁴⁷, S. Farry⁵⁴,
 431 D. Fazzini^{21,i}, L. Federici²⁵, D. Ferguson⁵², G. Fernandez³⁸, P. Fernandez Declara⁴⁰,
 432 A. Fernandez Prieto³⁹, F. Ferrari¹⁵, F. Ferreira Rodrigues², M. Ferro-Luzzi⁴⁰, S. Filippov³⁴,
 433 R.A. Fini¹⁴, M. Fiorini^{17,g}, M. Firlej²⁸, C. Fitzpatrick⁴¹, T. Fiutowski²⁸, F. Fleuret^{7,b},
 434 K. Fohl⁴⁰, M. Fontana^{16,40}, F. Fontanelli^{20,h}, D.C. Forshaw⁶¹, R. Forty⁴⁰, V. Franco Lima⁵⁴,
 435 M. Frank⁴⁰, C. Frei⁴⁰, J. Fu^{22,q}, W. Funk⁴⁰, E. Furfaro^{25,j}, C. Färber⁴⁰, E. Gabriel⁵²,
 436 A. Gallas Torreira³⁹, D. Galli^{15,e}, S. Gallorini²³, S. Gambetta⁵², M. Gandelman², P. Gandini²²,
 437 Y. Gao³, L.M. Garcia Martin⁷⁰, J. García Pardiñas³⁹, J. Garra Tico⁴⁹, L. Garrido³⁸,
 438 P.J. Garsed⁴⁹, D. Gascon³⁸, C. Gaspar⁴⁰, L. Gavardi¹⁰, G. Gazzoni⁵, D. Gerick¹²,
 439 E. Gersabeck⁵⁶, M. Gersabeck⁵⁶, T. Gershon⁵⁰, Ph. Ghez⁴, S. Giani⁴¹, V. Gibson⁴⁹,
 440 O.G. Girard⁴¹, L. Giubega³⁰, K. Gizdov⁵², V.V. Gligorov⁸, D. Golubkov³², A. Golutvin⁵⁵,
 441 A. Gomes^{1,a}, I.V. Gorelov³³, C. Gotti^{21,i}, E. Govorkova⁴³, J.P. Grabowski¹², R. Graciani Diaz³⁸,

442 L.A. Granado Cardoso⁴⁰, E. Graugés³⁸, E. Graverini⁴², G. Graziani¹⁸, A. Grecu³⁰, R. Greim⁹,
 443 P. Griffith¹⁶, L. Grillo²¹, L. Gruber⁴⁰, B.R. Gruberg Cazon⁵⁷, O. Grünberg⁶⁷, E. Gushchin³⁴,
 444 Yu. Guz³⁷, T. Gys⁴⁰, C. Göbel⁶², T. Hadavizadeh⁵⁷, C. Hadjivasiliou⁵, G. Haefeli⁴¹, C. Haen⁴⁰,
 445 S.C. Haines⁴⁹, B. Hamilton⁶⁰, X. Han¹², T.H. Hancock⁵⁷, S. Hansmann-Menzemer¹²,
 446 N. Harnew⁵⁷, S.T. Harnew⁴⁸, C. Hasse⁴⁰, M. Hatch⁴⁰, J. He⁶³, M. Hecker⁵⁵, K. Heinicke¹⁰,
 447 A. Heister⁹, K. Hennessy⁵⁴, P. Henrard⁵, L. Henry⁷⁰, E. van Herwijnen⁴⁰, M. Heß⁶⁷,
 448 A. Hicheur², D. Hill⁵⁷, C. Hombach⁵⁶, P.H. Hopchev⁴¹, W. Hu⁶⁵, Z.C. Huard⁵⁹,
 449 W. Hulsbergen⁴³, T. Humair⁵⁵, M. Hushchyn³⁵, D. Hutchcroft⁵⁴, P. Ibis¹⁰, M. Idzik²⁸, P. Ilten⁵⁸,
 450 R. Jacobsson⁴⁰, J. Jalocha⁵⁷, E. Jans⁴³, A. Jawahery⁶⁰, F. Jiang³, M. John⁵⁷, D. Johnson⁴⁰,
 451 C.R. Jones⁴⁹, C. Joram⁴⁰, B. Jost⁴⁰, N. Jurik⁵⁷, S. Kandybei⁴⁵, M. Karacson⁴⁰, J.M. Kariuki⁴⁸,
 452 S. Karodia⁵³, N. Kazeev³⁵, M. Kecke¹², F. Keizer⁴⁹, M. Kelsey⁶¹, M. Kenzie⁴⁹, T. Ketel⁴⁴,
 453 E. Khairullin³⁵, B. Khanji¹², C. Khurewathanakul⁴¹, T. Kirn⁹, S. Klaver⁵⁶, K. Klimaszewski²⁹,
 454 T. Klimkovich¹¹, S. Koliiev⁴⁶, M. Kolpin¹², R. Kopecna¹², P. Koppenburg⁴³, A. Kosmyntseva³²,
 455 S. Kotriakhova³¹, M. Kozeiha⁵, L. Kravchuk³⁴, M. Kreps⁵⁰, F. Kress⁵⁵, P. Krokovny^{36,w},
 456 F. Kruse¹⁰, W. Krzemien²⁹, W. Kucewicz^{27,l}, M. Kucharczyk²⁷, V. Kudryavtsev^{36,w},
 457 A.K. Kuonen⁴¹, T. Kvaratskheliya^{32,40}, D. Lacarrere⁴⁰, G. Lafferty⁵⁶, A. Lai¹⁶, G. Lanfranchi¹⁹,
 458 C. Langenbruch⁹, T. Latham⁵⁰, C. Lazzeroni⁴⁷, R. Le Gac⁶, A. Leflat^{33,40}, J. Lefrançois⁷,
 459 R. Lefèvre⁵, F. Lemaître⁴⁰, E. Lemos Cid³⁹, O. Leroy⁶, T. Lesiak²⁷, B. Leverington¹², P.-R. Li⁶³,
 460 T. Li³, Y. Li⁷, Z. Li⁶¹, T. Likhomanenko⁶⁸, R. Lindner⁴⁰, F. Lionetto⁴², V. Lisovskyi⁷, X. Liu³,
 461 D. Loh⁵⁰, A. Loi¹⁶, I. Longstaff⁵³, J.H. Lopes², D. Lucchesi^{23,o}, M. Lucio Martinez³⁹, H. Luo⁵²,
 462 A. Lupato²³, E. Luppi^{17,g}, O. Lupton⁴⁰, A. Lusiani²⁴, X. Lyu⁶³, F. Machefert⁷, F. Maciuc³⁰,
 463 V. Macko⁴¹, P. Mackowiak¹⁰, S. Maddrell-Mander⁴⁸, O. Maev^{31,40}, K. Maguire⁵⁶,
 464 D. Maisuzenko³¹, M.W. Majewski²⁸, S. Malde⁵⁷, B. Malecki²⁷, A. Malinin⁶⁸, T. Maltsev^{36,w},
 465 G. Manca^{16,f}, G. Mancinelli⁶, D. Marangotto^{22,q}, J. Maratas^{5,v}, J.F. Marchand⁴, U. Marconi¹⁵,
 466 C. Marin Benito³⁸, M. Marinangeli⁴¹, P. Marino⁴¹, J. Marks¹², G. Martellotti²⁶, M. Martin⁶,
 467 M. Martinelli⁴¹, D. Martinez Santos³⁹, F. Martinez Vidal⁷⁰, L.M. Massacrier⁷, A. Massafferri¹,
 468 R. Matev⁴⁰, A. Mathad⁵⁰, Z. Mathe⁴⁰, C. Matteuzzi²¹, A. Mauri⁴², E. Maurice^{7,b}, B. Maurin⁴¹,
 469 A. Mazurov⁴⁷, M. McCann^{55,40}, A. McNab⁵⁶, R. McNulty¹³, J.V. Mead⁵⁴, B. Meadows⁵⁹,
 470 C. Meaux⁶, F. Meier¹⁰, N. Meinert⁶⁷, D. Melnychuk²⁹, M. Merk⁴³, A. Merli^{22,40,q},
 471 E. Michielin²³, D.A. Milanese⁶⁶, E. Millard⁵⁰, M.-N. Minard⁴, L. Minzoni¹⁷, D.S. Mitzel¹²,
 472 A. Mogini⁸, J. Molina Rodriguez¹, T. Mombächer¹⁰, I.A. Monroy⁶⁶, S. Monteil⁵,
 473 M. Morandin²³, M.J. Morello^{24,t}, O. Morgunova⁶⁸, J. Moron²⁸, A.B. Morris⁵², R. Mountain⁶¹,
 474 F. Muheim⁵², M. Mulder⁴³, D. Müller⁵⁶, J. Müller¹⁰, K. Müller⁴², V. Müller¹⁰, P. Naik⁴⁸,
 475 T. Nakada⁴¹, R. Nandakumar⁵¹, A. Nandi⁵⁷, I. Nasteva², M. Needham⁵², N. Neri^{22,40},
 476 S. Neubert¹², N. Neufeld⁴⁰, M. Neuner¹², T.D. Nguyen⁴¹, C. Nguyen-Mau^{41,n}, S. Nieswand⁹,
 477 R. Niet¹⁰, N. Nikitin³³, T. Nikodem¹², A. Nogay⁶⁸, D.P. O’Hanlon⁵⁰, A. Oblakowska-Mucha²⁸,
 478 V. Obraztsov³⁷, S. Ogilvy¹⁹, R. Oldeman^{16,f}, C.J.G. Onderwater⁷¹, A. Ossowska²⁷,
 479 J.M. Otalora Goicochea², P. Owen⁴², A. Oyanguren⁷⁰, P.R. Pais⁴¹, A. Palano¹⁴,
 480 M. Palutan^{19,40}, A. Papanestis⁵¹, M. Pappagallo^{14,d}, L.L. Pappalardo^{17,g}, W. Parker⁶⁰,
 481 C. Parkes⁵⁶, G. Passaleva^{18,40}, A. Pastore^{14,d}, M. Patel⁵⁵, C. Patrignani^{15,e}, A. Pearce⁴⁰,
 482 A. Pellegrino⁴³, G. Penso²⁶, M. Pepe Altarelli⁴⁰, S. Perazzini⁴⁰, P. Perret⁵, L. Pescatore⁴¹,
 483 K. Petridis⁴⁸, A. Petrolini^{20,h}, A. Petrov⁶⁸, M. Petruzzo^{22,q}, E. Picatoste Olloqui³⁸,
 484 B. Pietrzyk⁴, M. Pikies²⁷, D. Pinci²⁶, F. Pisani⁴⁰, A. Pistone^{20,h}, A. Piucci¹², V. Placinta³⁰,
 485 S. Playfer⁵², M. Plo Casasus³⁹, F. Polci⁸, M. Poli Lener¹⁹, A. Poluektov⁵⁰, I. Polyakov⁶¹,
 486 E. Polcarpo², G.J. Pomery⁴⁸, S. Ponce⁴⁰, A. Popov³⁷, D. Popov^{11,40}, S. Poslavskii³⁷,
 487 C. Potterat², E. Price⁴⁸, J. Prisciandaro³⁹, C. Prouve⁴⁸, V. Pugatch⁴⁶, A. Puig Navarro⁴²,
 488 H. Pullen⁵⁷, G. Punzi^{24,p}, W. Qian⁵⁰, R. Quagliani^{7,48}, B. Quintana⁵, B. Rachwal²⁸,
 489 J.H. Rademacker⁴⁸, M. Rama²⁴, M. Ramos Pernas³⁹, M.S. Rangel², I. Raniuk^{45,†},
 490 F. Ratnikov³⁵, G. Raven⁴⁴, M. Ravonel Salzgeber⁴⁰, M. Reboud⁴, F. Redi⁵⁵, S. Reichert¹⁰,
 491 A.C. dos Reis¹, C. Remon Alepuz⁷⁰, V. Renaudin⁷, S. Ricciardi⁵¹, S. Richards⁴⁸, M. Rihl⁴⁰,

492 K. Rinnert⁵⁴, V. Rives Molina³⁸, P. Robbe⁷, A. Robert⁸, A.B. Rodrigues¹, E. Rodrigues⁵⁹,
 493 J.A. Rodriguez Lopez⁶⁶, A. Rogozhnikov³⁵, S. Roiser⁴⁰, A. Rollings⁵⁷, V. Romanovskiy³⁷,
 494 A. Romero Vidal³⁹, J.W. Ronayne¹³, M. Rotondo¹⁹, M.S. Rudolph⁶¹, T. Ruf⁴⁰, P. Ruiz Valls⁷⁰,
 495 J. Ruiz Vidal⁷⁰, J.J. Saborido Silva³⁹, E. Sadykhov³², N. Sagidova³¹, B. Saitta^{16,f},
 496 V. Salustino Guimaraes⁶², C. Sanchez Mayordomo⁷⁰, B. Sanmartin Sedes³⁹, R. Santacesaria²⁶,
 497 C. Santamarina Rios³⁹, M. Santimaria¹⁹, E. Santovetti^{25,j}, G. Sarpis⁵⁶, A. Sarti^{19,k},
 498 C. Satriano^{26,s}, A. Satta²⁵, D.M. Saunders⁴⁸, D. Savrina^{32,33}, S. Schael⁹, M. Schellenberg¹⁰,
 499 M. Schiller⁵³, H. Schindler⁴⁰, M. Schmelling¹¹, T. Schmelzer¹⁰, B. Schmidt⁴⁰, O. Schneider⁴¹,
 500 A. Schopper⁴⁰, H.F. Schreiner⁵⁹, M. Schubiger⁴¹, M.-H. Schune⁷, R. Schwemmer⁴⁰,
 501 B. Sciascia¹⁹, A. Sciubba^{26,k}, A. Semennikov³², E.S. Sepulveda⁸, A. Sergi⁴⁷, N. Serra⁴²,
 502 J. Serrano⁶, L. Sestini²³, P. Seyfert⁴⁰, M. Shapkin³⁷, I. Shapoval⁴⁵, Y. Shcheglov³¹, T. Shears⁵⁴,
 503 L. Shekhtman^{36,w}, V. Shevchenko⁶⁸, B.G. Siddi¹⁷, R. Silva Coutinho⁴², L. Silva de Oliveira²,
 504 G. Simi^{23,o}, S. Simone^{14,d}, M. Sirendi⁴⁹, N. Skidmore⁴⁸, T. Skwarnicki⁶¹, E. Smith⁵⁵,
 505 I.T. Smith⁵², J. Smith⁴⁹, M. Smith⁵⁵, I. Soares Lavra¹, M.D. Sokoloff⁵⁹, F.J.P. Soler⁵³,
 506 B. Souza De Paula², B. Spaan¹⁰, P. Spradlin⁵³, S. Sridharan⁴⁰, F. Stagni⁴⁰, M. Stahl¹²,
 507 S. Stahl⁴⁰, P. Stefko⁴¹, S. Stefkova⁵⁵, O. Steinkamp⁴², S. Stemmler¹², O. Stenyakin³⁷,
 508 M. Stepanova³¹, H. Stevens¹⁰, S. Stone⁶¹, B. Storaci⁴², S. Stracka^{24,p}, M.E. Stramaglia⁴¹,
 509 M. Straticiuc³⁰, U. Straumann⁴², J. Sun³, L. Sun⁶⁴, W. Sutcliffe⁵⁵, K. Swientek²⁸,
 510 V. Syropoulos⁴⁴, T. Szumlak²⁸, M. Szymanski⁶³, S. T'Jampens⁴, A. Tayduganov⁶,
 511 T. Tekampe¹⁰, G. Tellarini^{17,g}, F. Teubert⁴⁰, E. Thomas⁴⁰, J. van Tilburg⁴³, M.J. Tilley⁵⁵,
 512 V. Tisserand⁴, M. Tobin⁴¹, S. Tolk⁴⁹, L. Tomassetti^{17,g}, D. Tonelli²⁴, F. Toriello⁶¹,
 513 R. Tourinho Jadallah Aoude¹, E. Tournefier⁴, M. Traill⁵³, M.T. Tran⁴¹, M. Tresch⁴²,
 514 A. Trisovic⁴⁰, A. Tsaregorodtsev⁶, P. Tsopelas⁴³, A. Tully⁴⁹, N. Tuning^{43,40}, A. Ukleja²⁹,
 515 A. Usachov⁷, A. Ustyuzhanin³⁵, U. Uwer¹², C. Vacca^{16,f}, A. Vagner⁶⁹, V. Vagnoni^{15,40},
 516 A. Valassi⁴⁰, S. Valat⁴⁰, G. Valenti¹⁵, R. Vazquez Gomez⁴⁰, P. Vazquez Regueiro³⁹, S. Vecchi¹⁷,
 517 M. van Veghel⁴³, J.J. Velthuis⁴⁸, M. Veltri^{18,r}, G. Veneziano⁵⁷, A. Venkateswaran⁶¹,
 518 T.A. Verlage⁹, M. Vernet⁵, M. Vesterinen⁵⁷, J.V. Viana Barbosa⁴⁰, B. Viaud⁷, D. Vieira⁶³,
 519 M. Vieites Diaz³⁹, H. Viemann⁶⁷, X. Vilasis-Cardona^{38,m}, M. Vitti⁴⁹, V. Volkov³³,
 520 A. Vollhardt⁴², B. Voneki⁴⁰, A. Vorobyev³¹, V. Vorobyev^{36,w}, C. Voß⁹, J.A. de Vries⁴³,
 521 C. Vázquez Sierra³⁹, R. Waldi⁶⁷, C. Wallace⁵⁰, R. Wallace¹³, J. Walsh²⁴, J. Wang⁶¹,
 522 D.R. Ward⁴⁹, H.M. Wark⁵⁴, N.K. Watson⁴⁷, D. Websdale⁵⁵, A. Weiden⁴², C. Weisser⁵⁸,
 523 M. Whitehead⁴⁰, J. Wicht⁵⁰, G. Wilkinson⁵⁷, M. Wilkinson⁶¹, M. Williams⁵⁶, M.P. Williams⁴⁷,
 524 M. Williams⁵⁸, T. Williams⁴⁷, F.F. Wilson^{51,40}, J. Wimberley⁶⁰, M. Winn⁷, J. Wishahi¹⁰,
 525 W. Wislicki²⁹, M. Witek²⁷, G. Wormser⁷, S.A. Wotton⁴⁹, K. Wraight⁵³, K. Wyllie⁴⁰, Y. Xie⁶⁵,
 526 M. Xu⁶⁵, Z. Xu⁴, Z. Yang³, Z. Yang⁶⁰, Y. Yao⁶¹, H. Yin⁶⁵, J. Yu⁶⁵, X. Yuan⁶¹,
 527 O. Yushchenko³⁷, K.A. Zarebski⁴⁷, M. Zavertyaev^{11,c}, L. Zhang³, Y. Zhang⁷, A. Zhelezov¹²,
 528 Y. Zheng⁶³, X. Zhu³, V. Zhukov³³, J.B. Zonneveld⁵², S. Zucchelli¹⁵.

529 ¹Centro Brasileiro de Pesquisas Físicas (CBPF), Rio de Janeiro, Brazil

530 ²Universidade Federal do Rio de Janeiro (UFRJ), Rio de Janeiro, Brazil

531 ³Center for High Energy Physics, Tsinghua University, Beijing, China

532 ⁴LAPP, Université Savoie Mont-Blanc, CNRS/IN2P3, Annecy-Le-Vieux, France

533 ⁵Clermont Université, Université Blaise Pascal, CNRS/IN2P3, LPC, Clermont-Ferrand, France

534 ⁶Aix Marseille Univ, CNRS/IN2P3, CPPM, Marseille, France

535 ⁷LAL, Univ. Paris-Sud, CNRS/IN2P3, Université Paris-Saclay, Orsay, France

536 ⁸LPNHE, Université Pierre et Marie Curie, Université Paris Diderot, CNRS/IN2P3, Paris, France

537 ⁹I. Physikalisches Institut, RWTH Aachen University, Aachen, Germany

538 ¹⁰Fakultät Physik, Technische Universität Dortmund, Dortmund, Germany

539 ¹¹Max-Planck-Institut für Kernphysik (MPIK), Heidelberg, Germany

540 ¹²Physikalisches Institut, Ruprecht-Karls-Universität Heidelberg, Heidelberg, Germany

541 ¹³School of Physics, University College Dublin, Dublin, Ireland

542 ¹⁴Sezione INFN di Bari, Bari, Italy

543 ¹⁵ *Sezione INFN di Bologna, Bologna, Italy*
544 ¹⁶ *Sezione INFN di Cagliari, Cagliari, Italy*
545 ¹⁷ *Universita e INFN, Ferrara, Ferrara, Italy*
546 ¹⁸ *Sezione INFN di Firenze, Firenze, Italy*
547 ¹⁹ *Laboratori Nazionali dell'INFN di Frascati, Frascati, Italy*
548 ²⁰ *Sezione INFN di Genova, Genova, Italy*
549 ²¹ *Universita e INFN, Milano-Bicocca, Milano, Italy*
550 ²² *Sezione di Milano, Milano, Italy*
551 ²³ *Sezione INFN di Padova, Padova, Italy*
552 ²⁴ *Sezione INFN di Pisa, Pisa, Italy*
553 ²⁵ *Sezione INFN di Roma Tor Vergata, Roma, Italy*
554 ²⁶ *Sezione INFN di Roma La Sapienza, Roma, Italy*
555 ²⁷ *Henryk Niewodniczanski Institute of Nuclear Physics Polish Academy of Sciences, Kraków, Poland*
556 ²⁸ *AGH - University of Science and Technology, Faculty of Physics and Applied Computer Science, Kraków, Poland*
557 ²⁹ *National Center for Nuclear Research (NCBJ), Warsaw, Poland*
558 ³⁰ *Horia Hulubei National Institute of Physics and Nuclear Engineering, Bucharest-Magurele, Romania*
559 ³¹ *Petersburg Nuclear Physics Institute (PNPI), Gatchina, Russia*
560 ³² *Institute of Theoretical and Experimental Physics (ITEP), Moscow, Russia*
561 ³³ *Institute of Nuclear Physics, Moscow State University (SINP MSU), Moscow, Russia*
562 ³⁴ *Institute for Nuclear Research of the Russian Academy of Sciences (INR RAN), Moscow, Russia*
563 ³⁵ *Yandex School of Data Analysis, Moscow, Russia*
564 ³⁶ *Budker Institute of Nuclear Physics (SB RAS), Novosibirsk, Russia*
565 ³⁷ *Institute for High Energy Physics (IHEP), Protvino, Russia*
566 ³⁸ *ICCUB, Universitat de Barcelona, Barcelona, Spain*
567 ³⁹ *Universidad de Santiago de Compostela, Santiago de Compostela, Spain*
568 ⁴⁰ *European Organization for Nuclear Research (CERN), Geneva, Switzerland*
569 ⁴¹ *Institute of Physics, Ecole Polytechnique Fédérale de Lausanne (EPFL), Lausanne, Switzerland*
570 ⁴² *Physik-Institut, Universität Zürich, Zürich, Switzerland*
571 ⁴³ *Nikhef National Institute for Subatomic Physics, Amsterdam, The Netherlands*
572 ⁴⁴ *Nikhef National Institute for Subatomic Physics and VU University Amsterdam, Amsterdam, The Netherlands*
573 ⁴⁵ *NSC Kharkiv Institute of Physics and Technology (NSC KIPT), Kharkiv, Ukraine*
574 ⁴⁶ *Institute for Nuclear Research of the National Academy of Sciences (KINR), Kyiv, Ukraine*
575 ⁴⁷ *University of Birmingham, Birmingham, United Kingdom*
576 ⁴⁸ *H.H. Wills Physics Laboratory, University of Bristol, Bristol, United Kingdom*
577 ⁴⁹ *Cavendish Laboratory, University of Cambridge, Cambridge, United Kingdom*
578 ⁵⁰ *Department of Physics, University of Warwick, Coventry, United Kingdom*
579 ⁵¹ *STFC Rutherford Appleton Laboratory, Didcot, United Kingdom*
580 ⁵² *School of Physics and Astronomy, University of Edinburgh, Edinburgh, United Kingdom*
581 ⁵³ *School of Physics and Astronomy, University of Glasgow, Glasgow, United Kingdom*
582 ⁵⁴ *Oliver Lodge Laboratory, University of Liverpool, Liverpool, United Kingdom*
583 ⁵⁵ *Imperial College London, London, United Kingdom*
584 ⁵⁶ *School of Physics and Astronomy, University of Manchester, Manchester, United Kingdom*
585 ⁵⁷ *Department of Physics, University of Oxford, Oxford, United Kingdom*
586 ⁵⁸ *Massachusetts Institute of Technology, Cambridge, MA, United States*
587 ⁵⁹ *University of Cincinnati, Cincinnati, OH, United States*
588 ⁶⁰ *University of Maryland, College Park, MD, United States*
589 ⁶¹ *Syracuse University, Syracuse, NY, United States*
590 ⁶² *Pontifícia Universidade Católica do Rio de Janeiro (PUC-Rio), Rio de Janeiro, Brazil, associated to ²*
591 ⁶³ *University of Chinese Academy of Sciences, Beijing, China, associated to ³*
592 ⁶⁴ *School of Physics and Technology, Wuhan University, Wuhan, China, associated to ³*
593 ⁶⁵ *Institute of Particle Physics, Central China Normal University, Wuhan, Hubei, China, associated to ³*
594 ⁶⁶ *Departamento de Física, Universidad Nacional de Colombia, Bogota, Colombia, associated to ⁸*
595 ⁶⁷ *Institut für Physik, Universität Rostock, Rostock, Germany, associated to ¹²*
596 ⁶⁸ *National Research Centre Kurchatov Institute, Moscow, Russia, associated to ³²*

599 ⁶⁹ *National Research Tomsk Polytechnic University, Tomsk, Russia, associated to* ³²
600 ⁷⁰ *Instituto de Fisica Corpuscular, Centro Mixto Universidad de Valencia - CSIC, Valencia, Spain,*
601 *associated to* ³⁸
602 ⁷¹ *Van Swinderen Institute, University of Groningen, Groningen, The Netherlands, associated to* ⁴³

603 ^a *Universidade Federal do Triângulo Mineiro (UFTM), Uberaba-MG, Brazil*
604 ^b *Laboratoire Leprince-Ringuet, Palaiseau, France*
605 ^c *P.N. Lebedev Physical Institute, Russian Academy of Science (LPI RAS), Moscow, Russia*
606 ^d *Università di Bari, Bari, Italy*
607 ^e *Università di Bologna, Bologna, Italy*
608 ^f *Università di Cagliari, Cagliari, Italy*
609 ^g *Università di Ferrara, Ferrara, Italy*
610 ^h *Università di Genova, Genova, Italy*
611 ⁱ *Università di Milano Bicocca, Milano, Italy*
612 ^j *Università di Roma Tor Vergata, Roma, Italy*
613 ^k *Università di Roma La Sapienza, Roma, Italy*
614 ^l *AGH - University of Science and Technology, Faculty of Computer Science, Electronics and*
615 *Telecommunications, Kraków, Poland*
616 ^m *LIFAEELS, La Salle, Universitat Ramon Llull, Barcelona, Spain*
617 ⁿ *Hanoi University of Science, Hanoi, Viet Nam*
618 ^o *Università di Padova, Padova, Italy*
619 ^p *Università di Pisa, Pisa, Italy*
620 ^q *Università degli Studi di Milano, Milano, Italy*
621 ^r *Università di Urbino, Urbino, Italy*
622 ^s *Università della Basilicata, Potenza, Italy*
623 ^t *Scuola Normale Superiore, Pisa, Italy*
624 ^u *Università di Modena e Reggio Emilia, Modena, Italy*
625 ^v *Iligan Institute of Technology (IIT), Iligan, Philippines*
626 ^w *Novosibirsk State University, Novosibirsk, Russia*

627 [†] *Deceased*